Experimental and Numerical Analysis of the Hydrodynamic Behaviors of Aerobic Granules

Li Liu and Guo-Ping Sheng*
School of Earth and Space Sciences, University of Science and Technology of China, Hefei, 230026, China

Wen-Wei Li, Raymond J. Zeng, and Han-Qing Yu
Dept. of Chemistry, University of Science and Technology of China, Hefei, 230026, China

DOI 10.1002/aic.12476
Published online November 29, 2010 in Wiley Online Library (wileyonlinelibrary.com).

Aerobic granular sludge has been recognized to be promising for wastewater treatment. Their hydrodynamic characteristics have a significant impact on the mass transfer process in reactors. In this study, the hydrodynamic characteristics of aerobic granules were studied using an experimental approach, and their fluid dynamic behaviors were analyzed using a numerical approach. Experimental results show that the aerobic granules are fractal-like aggregates with porosity. Their porosity and permeability were found to increase with increasing granule size. The numerical model simulated the flow field surrounding a granule, which distinguished the flow behaviors of the granules with different permeability at different outflow Reynolds numbers. The velocity vectors colored by velocity magnitude in the granule internal depended significantly on the permeability of the granule and the Reynolds number. The results provided a helpful tool to investigate the hydrodynamic behavior of aerobic granules with a consideration of their porous structure characteristics. © 2010 American Institute of Chemical Engineers *AIChE J,* 57: 2909–2916, 2011

Keywords: aerobic granule, computational fluid dynamics, flow field, hydrodynamics, permeability, porosity, sequencing batch reactor, wastewater treatment

Introduction

Aerobic granular sludge has been recognized to be promising for wastewater treatment due to its many advantages over the conventional activated sludge flocs, such as good settling ability, high-biomass retention, and great capability to withstand shock loading.[1–6] The excellent properties of aerobic granules are related greatly with their internal structure. Their formation, structure, and mass transfer in granules are also influenced by the internal fluid patterns. It is found that aerobic granules are fractal-like aggregates composed by small particles.[7–10] For fractal aggregates, fractal dimension has been widely used to describe their irregular and complex structure, and it is useful in explaining some phenomena of aerobic granules.

The hydrodynamic behaviors of microbial aggregates could affect their mass-transfer efficiency and accordingly reactor performance.[11–13] Attempts have been made to analyze the hydrodynamic characteristics of granules. Su and Yu[10] studied the fractal dimension and the permeation of granules grown on the soybean-processing wastewater. They revealed that 83% of matured granules were permeable with fluid collection efficiencies over 0.034. Mu et al.[14] established a new approach to evaluate the drag coefficient of porous and permeable microbial granules, and demonstrated that the drag coefficient of microbial granules depended heavily on their permeable structure.

The increased capabilities of the computational fluid dynamics (CFD) make it possible to carry out CFD-based simulation of bioreactors.[15,16] Diez et al.[17] carried out

*Guo-Ping Sheng is also affliated with the Dept. of Chemistry.
Correspondence concerning this article should be addressed to G.-P. Sheng at gpsheng@ustc.edu.cn.

experimental, CFD simulation and artificial neuronal network studies to analyze the fluid mechanism of the aerobic granules cultivated in a sequencing batch reactor (SBR). Ren et al.[18] performed a three-dimensional CFD simulation with an Eulerian–Eulerian three-phase-fluid approach to visualize the phase holdup and flow patterns in upflow anaerobic sludge blanket reactors. However, in these studies, the whole reactor was investigated at a macroscopic level, which can not reflect the fluid forces imposed on granules at a microscopic level. There are an increasing number of processes involving hydrodynamic and mass transfer to viscous fluids, which demands further efforts to understand the effect of liquid viscosity on particle or bubble oscillations at different Reynolds.[19,20] The hydrodynamic behaviors of granules can significantly affect the mass transfer of oxygen and substrate. However, information about such hydrodynamic behaviors is still limited, attributed to the complex hydrodynamic conditions of the reactor and the porous structure of granules.

Therefore, in this study, the hydrodynamic characteristics of aerobic granules were investigated with integrated experimental and numerical approaches. The hydrodynamic parameters, e.g., the porosity, fractal dimension, and permeability of the granules, were experimentally determined. Then, the fluid dynamic behaviors such as the velocity field inside and outside the granule, path lines, and the granule shear rate were analyzed using the CFD modeling approach on the basis of granule hydrodynamic characteristics at different outflow Reynolds numbers (*Re*). Understanding the characteristics of the flow field of in aerobic-granule-based reactors is essential for a successful operation and scale-up of the bioreactors for wastewater treatment.

Model Development

Assumptions

In the CFD calculation, an aerobic granule is assumed as a porous sphere with a diameter d. It moves at a speed of u_8 through an infinitely large quiescent Newtonian fluid of viscosity μ and density ρ. The diameter (D_L) and the length (L) of the domain tube are kept as 60 times of the granule diameter ($d = 2\ r_g$) to minimize the boundary effects. Figure 1 illustrates the flow process: the sphere is fixed at the centerline, whereas the surrounding fluid flows at a uniform speed of u_8 from infinity toward the fixed sphere. The flow fields within and around the sphere should be modeled separately.

Governing equations and solutions

The governing equations for the flow field outside the permeable granule could be described by:

$$\left(\vec{u}'_{\mathrm{f}} \cdot \nabla\right)\vec{u}'_{\mathrm{f}} + \frac{P_0}{\rho V^2}\nabla P' = \frac{1}{Re}\nabla^2\vec{u}'_{\mathrm{f}} \tag{1}$$

where $\vec{u}'_{\mathrm{f}} = \vec{u}_{\mathrm{f}}/u_\infty$ and $P' = P/P_0$. The Re of granules could be calculated from:

$$\mathrm{Re} = \frac{d\rho u_\infty}{\mu} \tag{2}$$

The fluid flow interior to the granule is expressed by the Darcy-Brinkman's equation:

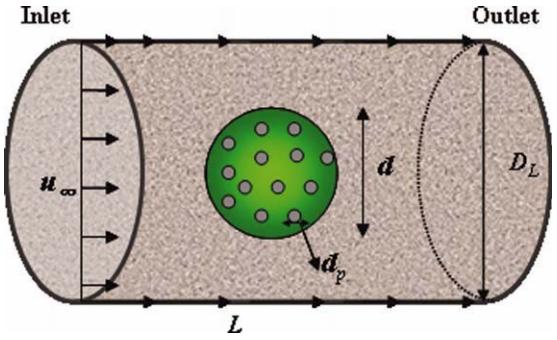

Figure 1. Computational domain under investigations (L/d = 60, D_L/d = 60).

[Color figure can be viewed in the online issue, which is available at wileyonlinelibrary.com.]

$$\vec{u}'_{\mathrm{p}} + \frac{Eu}{\beta^2}Re\nabla P' = \frac{1}{\beta}\nabla^2\vec{u}'_{\mathrm{p}} \tag{3}$$

where $\vec{u}'_{\mathrm{p}} = \vec{u}_{\mathrm{p}}/u_\infty$ and $Eu = P_0/\rho u_\infty^2$ (Euler number). The dimensionless permeability factor (β) of the granule is:

$$\beta = (d/2)/\kappa^{0.5} \tag{4}$$

where κ is the granule hydraulic permeability. The fluid viscosity of fluid interior to the granule is assumed to be the same as that of fluid exterior to it.[21]

The boundary conditions are defined as follows:

$$\vec{u}_{\mathrm{f}} = \vec{u}_\infty,\ r \to \infty \tag{5}$$

$$\vec{u}'_{\mathrm{p}} = \vec{u}'_{\mathrm{f}},\ r = r_{\mathrm{g}} \tag{6}$$

$$\nabla\vec{u}'_{\mathrm{p}} = \nabla\vec{u}'_{\mathrm{f}},\ r = r_{\mathrm{g}} \tag{7}$$

$$\frac{\partial\bar{u}_p}{\partial r} = \frac{\partial\bar{u}_f}{\partial r} = \bar{0},\ r = 0 \tag{8}$$

Equation 5 implies that at the point far away from a granule the flow field is not disturbed by the granule. Equations 6 and 7 indicate that both the fluid velocity and its gradient across the sphere surface are continuous.

For a specific granule moving in the water bath at a constant velocity, both the Euler number (Eu) and Re of the granule could be treated as known values in Eqs. 1 and 3. Hence, the fluid-flow field and the associated hydrodynamic drag are determined by a single parameter, β.

The relationship between the wet mass (W_{d}) of granule and its size (d) could be described as[22]:

$$W_{\mathrm{d}} = Ad^D \tag{9}$$

where the constant A and the fractal dimension of the granule D could be estimated from the slope and intercept of a log–log plot of the wet mass and size of granules, respectively.

The granule porosity (ε) is determined with the following equation:

$$\varepsilon = 1 - \frac{6fA}{\pi\rho_{\mathrm{g}}}d^{D-3} \tag{10}$$

where ρ_g is the density of granule, the ratio (f) is the wet mass to the dry mass of the granules, which is estimated to be 3.45 according to Li and Yuan.[23]

The Happel model is used to calculate the hydraulic permeability (κ) of aerobic granules[14]:

$$\kappa = \frac{d_p^2(3 - 4.5\gamma + 4.5\gamma^2 - 3\gamma^3)}{18\gamma^3(3 + 2\gamma^5)} \tag{11}$$

$$\gamma = (1 - \varepsilon)^{1/3} \tag{12}$$

where d_p is the primary particle diameter. In this study, three d_p values, i.e., 1, 5, and 10 μm, are selected according to Li and Ganczarczyk.[24]

Hydrodynamic shear forces play a crucial role in maintaining the integrity of aerobic granules, which has been confirmed for aerobic granulation.[1,2] The shear rate S (s^{-1}), which affects the deformation of granules in the fluid field due to the hydrodynamic shear forces, is defined based on the Euclidian norm of the deformation tensor:

$$S = \sqrt{2S_{ij}S_{ij}} \tag{13}$$

$$S_{ij} = \frac{1}{2}\left(\frac{\partial \vec{u}_i}{\partial x_j} + \frac{\partial \vec{u}_j}{\partial x_i}\right) \tag{14}$$

Numerical solution

The model in Figure 1 was initially preprocessed using the geometry modeling mesh generation software, GAMBIT 2.0 (Fluent, USA) to define the liquid–solid interface and to generate the outside flow field grids. The governing equations and the associated boundary conditions were solved numerically using FLUENT 6.2 software (Fluent, USA). In FLUENT simulation, the aerobic granule was defined as a porous zone and the permeability was decided by both porosity and size of the primary particles described above. The adopted pressure-velocity coupling algorithm was Semi-Implicit Method for Pressure-Linked Equations-Consistent (SIMPLEC). The calculation was performed at a maximum relative error of 0.01%.

Materials and Methods

Experimental setup

The SBR used to cultivate aerobic granules had an internal diameter of 0.1 m and a height of 1.0 m. The reactor was operated at 20°C with a total cycle length of 6-h mode, including: 3 min of feeding, 349 min of aeration, 1 min of settling, and 5 min of effluent withdrawal. Air was introduced through a diffuser at the reactor bottom by an air pump. The airflow rate was controlled via a flow meter. The seed sludge was taken from an aeration tank in Wangxiaoying Municipal Wastewater Treatment Plant, Hefei, China. The granules were cultivated by a diluted effluent from a laboratory scale H_2-producing upflow anaerobic reactor. The effluent was rich in volatile fatty acids, including acetate, propionate, and butyrate.[25] The influent chemical oxygen demand to the reactor was kept at $\sim$ 1000 mg L^{-1}. In addition, the micro-element solution of 1.0 mL L^{-1} was added, which contained (in mg L^{-1}): H_3BO_3, 50; $ZnCl_2$, 50; $CuCl_2$, 30; $MnSO_4{\cdot}H_2O$, 50; $(NH_4)_6MO_7O_{24}{\cdot}4H_2O$, 50; $AlCl_3$, 50; $CoCl_2{\cdot}6H_2O$, 50; and $NiCl_2$, 50. The influent pH value was adjusted to 7.0 through the dose of $NaHCO_3$ or HCl.

Analytical methods

The density (ρ_g) of the aerobic granules was determined according to Zheng et al.[4] The granule size was measured using an image analysis system (Image-pro Express 4.0, Media Cybernetics, USA) with an Olympus CX41 microscope and a digital camera (C5050, Olympus Co., Japan). The granules were dried in an oven with 101°C for 2 h and the dry mass (W_d) was weighed by an analytical balance. The settling velocity of granules was measured by recording the time taken for an individual granule to fall from a certain height in a measuring cylinder. A column with a diameter of 4.0 cm and a height of 40 cm was used for the measurement.[10]

The mixed liquor suspended solids (MLSS), sludge volume index (SVI), and specific gravity were determined following the Standard Methods.[26]

Results and Discussion

Morphology profiles

Morphology of the activated sludge in the SBR changed significantly during the granulation process (Figure 2). The seed sludge had an irregular and loose structure (Figure 2A). In Figure 2B, smaller aggregates could be seen after 5 days of operation. After 8 days, small granules with diameters of 0.2–0.5 mm were visible (Figure 2C). These small granules coexisted with flocs in the reactor as seen in Figure 2D. These initial granules grew rapidly and, after 10 more days, large granules with diameters over 1.0 mm were observed (Figure 2E). After 30 days of rapid growth, the growth rate of granules gradually slowed down, indicating the formation of mature and stable granules. The matured aerobic granules had a diameter ranging from 1.0 to 3.5 mm and SVI of 74.2 mL g^{-1}. With a shift from small and loose sludge flocs to large and dense granules, a stable and clear outer surface was gradually formed, indicating the development of a more compacted granule structure (Figure 2F).

Fractal porous structure

In this study, total of 65 aerobic granules was used for analysis and calculation. The sizes of the granules ranged from 1.0 to 3.5 mm with a dry mass from 0.012 to 0.533 mg. Fractal dimension can be used to describe the space filling capacity of an object, whereas Euclidean dimensions are integers varying from 0 to 3. For linear, planar, and three-dimensionally compact objects, the exponent D has values of 1, 2, and 3, respectively. Fractal geometry regards that, as opposed to the classical Euclidean geometry, the dimension of an object can be a noninteger value. It could provide a valuable indicator for the formation mechanisms and the

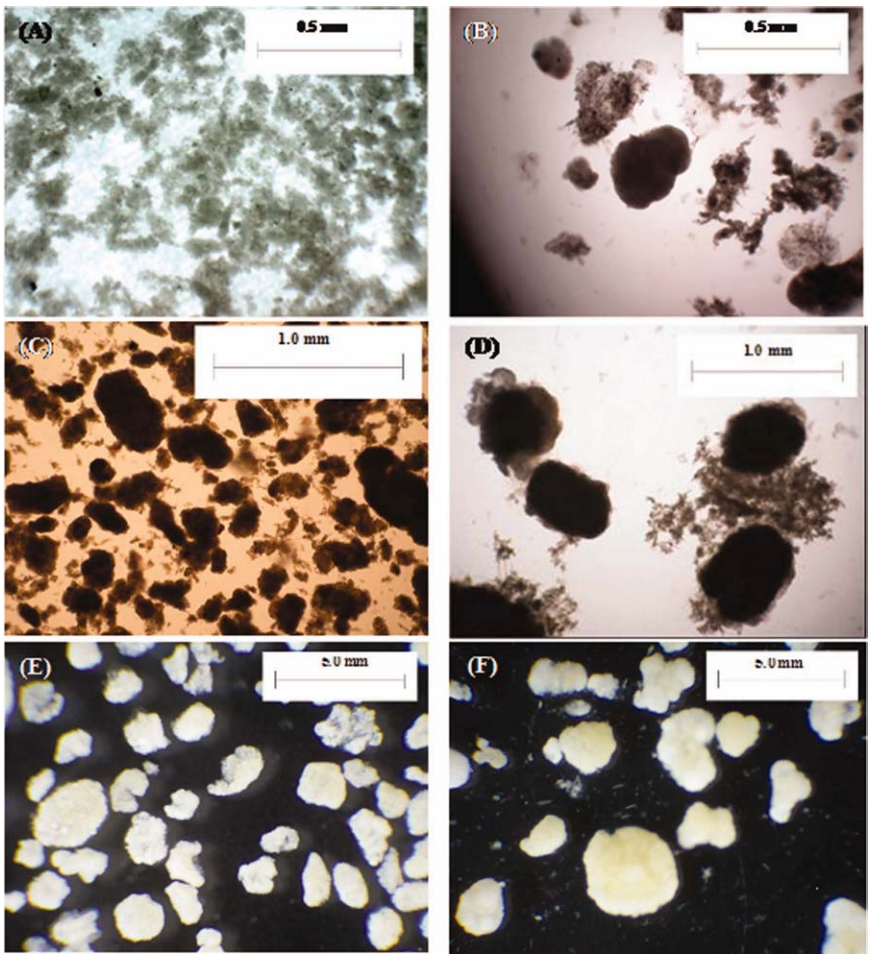

Figure 2. Images of sludge in the granulation process.

A: Seed sludge, (B) sludge on day 5, (C) sludge on day 8, (D) sludge on day 15, (E) sludge on day 20, and (F) sludge on day 34. [Color figure can be viewed in the online issue, which is available at wileyonlinelibrary.com.]

structural features of aerobic granules. Based on the slope of the logarithmic relationship between the dry mass (W_d) and size (d), the fractal dimension D of the aerobic granule was determined as 2.65 $\pm$ 0.19 ($r^2 = 0.913$), as shown in Figure 3A. This implies the granules had a fractal structure. Thus, Eq. 9 could be written as follows:

$$W_d = 0.0223d^{2.65} \tag{15}$$

For porous aggregates such as activated sludge flocs, the fractal values are typically in a relatively wide range of 1.4–2.8.[27] A lower fractal dimension value generally indicates a looser and more porous aggregate structure and thus better mass-transfer ability, whereas a higher fractal dimension suggests a denser and stronger structure formed under a highly sheared environment.[28]

As shown in Figure 3B, the granule porosity is related to its diameter. When the granule diameter increased from 1.0 to 3.5 mm, the porosity increased from 0.86 to 0.91, indicating that a larger granule generally had a more porous structure. The high-mass-transfer efficiency of a granule is usually associated with its porous structure, which allows the development of interior flow.[14]

Permeability

Happel model (Eq. 11) was adopted to estimate the permeability κ of the aerobic granules. As shown in Figure 4A, the κ value increased slightly with the increasing granule size and the primary particle diameter. For instance, the permeability of the granules with a primary particle size of 10 μm was almost 10 times higher than that of the granules with a primary particle size of 1 μm. These results show that the permeability of aerobic granules was related to their size and primary particle size. Fractal aggregates show a heterogeneous pore distribution, whereas the macropores formed between particles within an aggregates allow a greater interior flow through the aggregates.[22]

Figure 4B plots the permeability factor (β) as a function of Re and primary particle size d_p. For granules with different primary particle sizes, the β value increased with the Re value, especially for those with a larger d_p of 10 μm. When the external flow velocity increased, the intra-granule fluid flow would redistribute among the channels of different sizes, and yield a Re-dependent permeability. As for sludge flocs, which are highly porous aggregate,[28] the β value is usually very small, ranging from 1.4 to 6.8.[29] However, the β values of aerobic and anaerobic granules generally range from 10 to

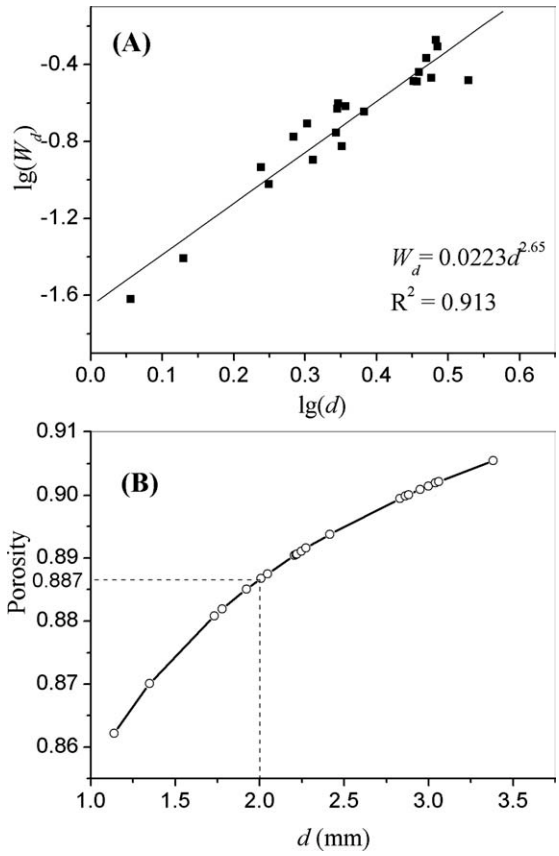

Figure 3. A: Fractal dimension and (B) porosity of the granules.

10,000.[14] This indicates that aerobic granules have more compact interior structure than flocs, which leads to an increased mass-transfer resistance to oxygen and nutrient intake.[30] The relationship between the permeability and the mass transport of aerobic granules needs further investigations.

Flow field surrounding granules at different Re *values*

The CFD model described above was used to evaluate the fluid mechanics behavior of a 2-mm granule. The hydrodynamic parameters of the granule, such as the porosity ($\varepsilon = 0.887$) and the permeability of two different primary particle size ($\kappa = 2.5$ E -13 for $d_p = 1$ μm, and $\kappa = 2.46$ E -11 for $d_p = 10$ μm), were obtained from the experimental results above. The fluid field characteristics, such as the velocity field, path lines, and the shear rate, are shown in Figures 5–7.

Figures 5A–H show the velocity field plots of a granule with d_p of 1 and 10 μm and *Re* value of 0.5, 1, 5, and 10, respectively. For a porous sphere, the fluid not only flows around but also penetrates through the sphere. This could be confirmed by the size exclusion chromatography method by Adav et al.,[30] which demonstrated a significant convection flow through the aerobic granule interior. The velocity vectors colored by velocity magnitude in the interior and around the granule exhibited a significant permeability-*Re* dependency. As shown in Figures 5A, B, a higher fraction of velocity vectors inside the granule with $d_p = 10$ μm were found than that for the granule with $d_p = 1$ μm at the same *Re* value, implying an elevated internal convection alone with the granule permeability. The velocity vectors inside the granule increased as the *Re* value increased from 0.5 to 10, suggesting that enhancement of the surrounding flow could increase the granule internal convection. The fluid field around the granule affected its internal convection, which exerted an influence on the mass-transfer efficiency of the granules. The convection inside granules could enhance the oxygen and substance transfer process of aerobic granules.

The change of the fluid field as the response to increasing *Re* values could be observed by the variations of the path lines around the granule. The path lines for the granule of $d_p = 1$ μm changed notably at *Re* values of 0.5, 5, 10, and 50 (Figures 6A–D). At *Re* of 0.5, the path lines paralleled nearly to the granule surface shape when passing through the granule. Meanwhile, the streamlines were almost symmetrical around the granule, as aerobic granules have a much higher β value than the usual microsphere aggregates.[14] As *Re* increased, the streamlines through the granule internal could be observed obviously. This further confirms that the external flow could affect the internal fluid field of the granule due to its porous structure.

In a bioreactor, the shear force resulting from fluid hydraulics is one of the key factors that influence the formation, structure, and stability of the cell-immobilization community, such as biofilm and granular sludge under different hydrodynamic conditions.[31] The shear rate of the aerobic granules with different d_p values in the flow fluid of different *Re* values are showed in Figure 7. The maximum strain rate appeared at the flank guard of the granule, whereas the minimum one appeared in the flow direction behind the granule in each

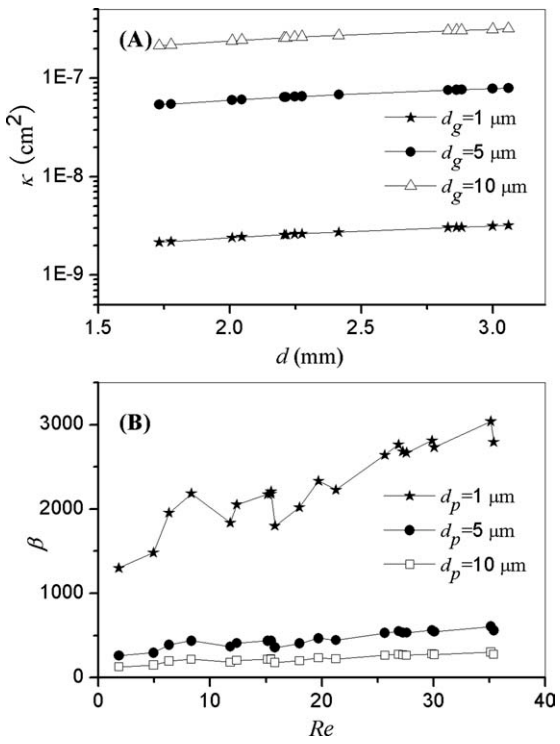

Figure 4. A: Permeability of the granules with different diameters and (B) dimensionless permeability factor β as a function of *Re* for the granules.

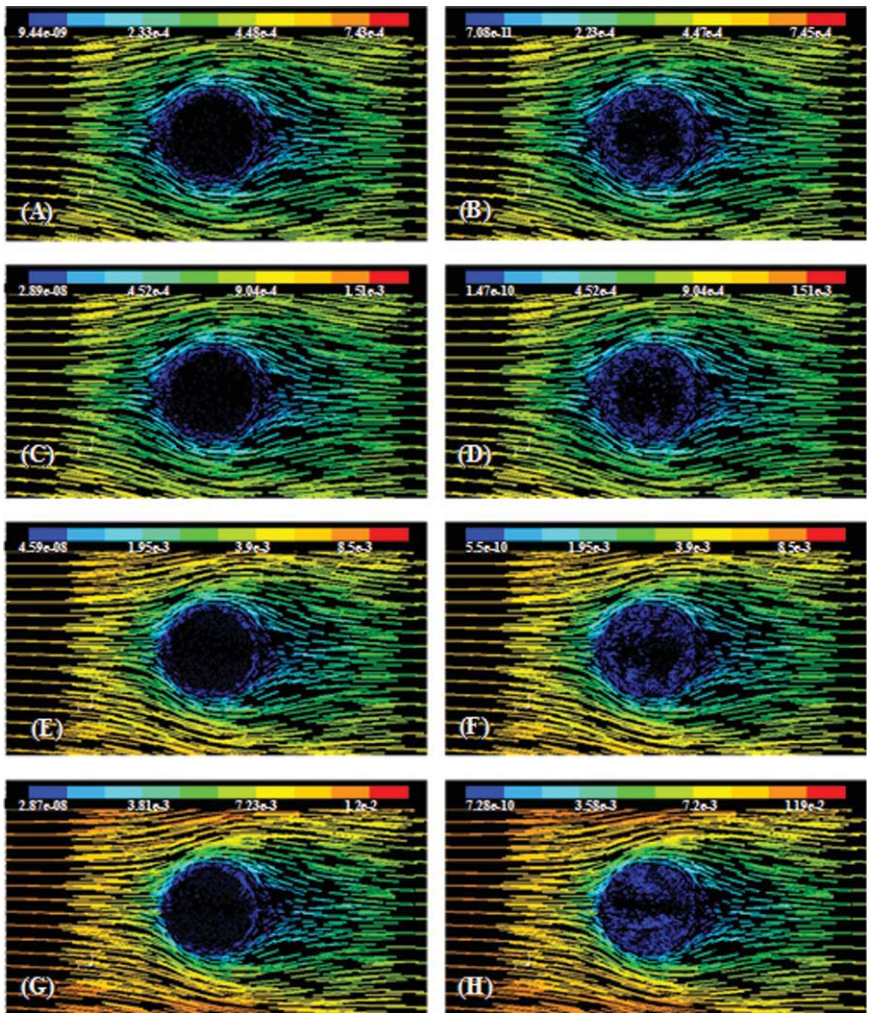

Figure 5. Velocity vectors colored by velocity magnitude (m s^{-1}) interior and around the granules of different d_p at different *Re*.

A: $Re = 0.5$, $d_p = 1$ μm; (B) $Re = 0.5$, $d_p = 10$ μm; (C) $Re = 1$, $d_p = 1$ μm; (D) $Re = 1$, $d_p = 10$ μm; (E) $Re = 5$, $d_p = 1$ μm; (F) $Re = 5$, $d_p = 10$ μm; (G) $Re = 10$, $d_p = 1$ μm; and (H) $Re = 10$, $d_p = 10$ μm. [Color figure can be viewed in the online issue, which is available at wileyonlinelibrary.com.]

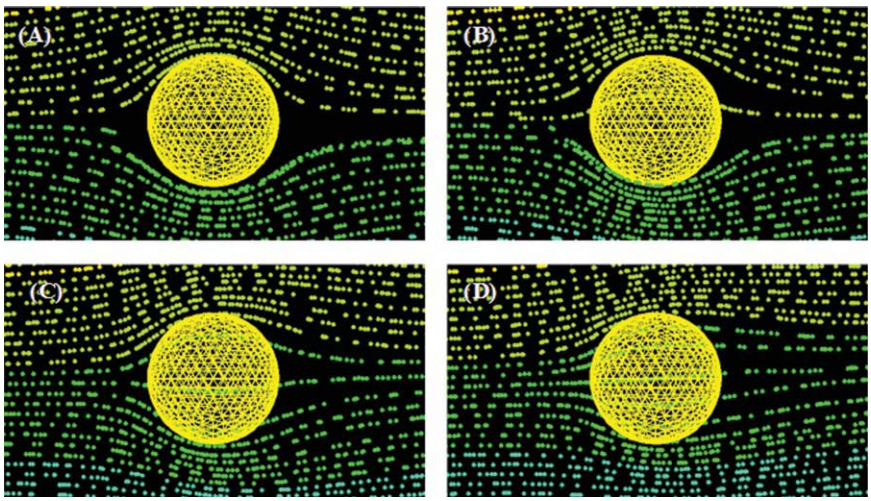

Figure 6. Path lines for the granule of $d_p = 1$ μm at: (A) *Re* = 0.5, (B) *Re* = 5, (C) *Re* = 10, and (D) *Re* = 50.

[Color figure can be viewed in the online issue, which is available at wileyonlinelibrary.com.]

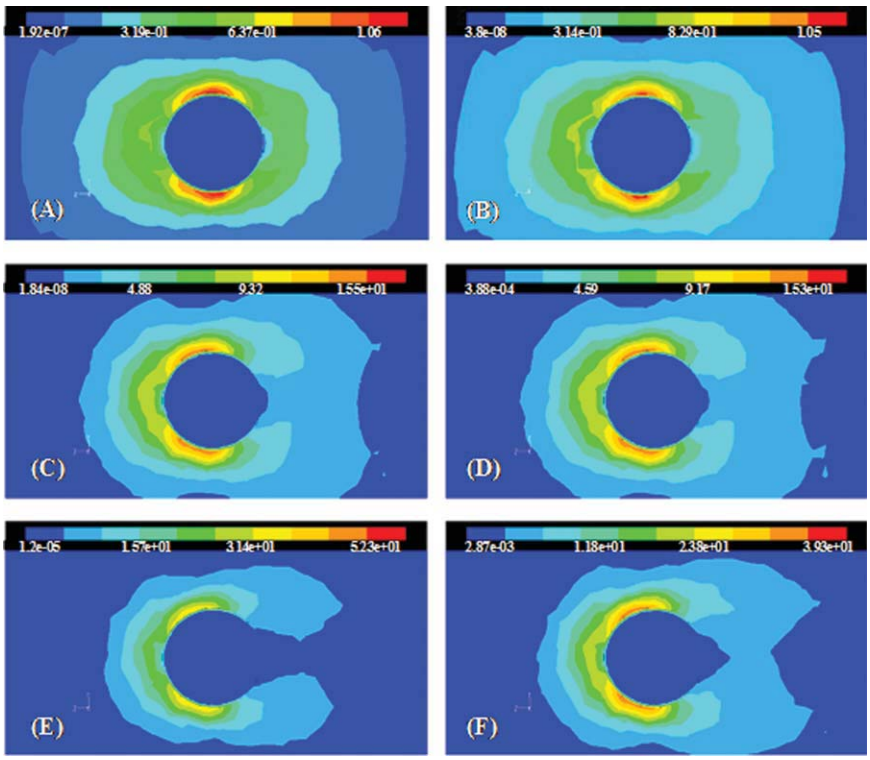

Figure 7. Strain rate of the aerobic granules with different d_p at different *Re*.

A: $Re = 0.5$, $d_p = 1$ μm; (B) $Re = 0.5$, $d_p = 10$ μm; (C) $Re = 5$, $d_p = 1$ μm; (D) $Re = 5$, $d_p = 10$ μm; (E) $Re = 10$, $d_p = 1$ μm; and (F) $Re = 10$, $d_p = 10$ μm. [Color figure can be viewed in the online issue, which is available at wileyonlinelibrary.com.]

calculated result. As the *Re* increased from 0.5 to 10, the maximum shear rate of granules with d_p of 1 μm increased from 1.06 to 52.3 s^{-1}, whereas that of the granules with d_p of 10 μm increased from 1.05 to 39.3 s^{-1}. At a small *Re* value, the shear rate difference between two granules was neglectable. However, after *Re* reached 50, the more permeable granules with d_p of 10 μm weighted a smaller shear rate compared with the granule with d_p of 1 μm. This suggests that the granule permeability is able to reduce the resistance brought by the surrounding flow to a certain degree.

Conclusions

In this study, the hydrodynamic behaviors of aerobic granules were studied using both experimental and numerical approaches. Results show that the aerobic granules had a porous and fractal structure. Their porosity and permeability were found to increase with the increasing granule size. The velocity field and the path lines obtained by the CFD model show that the enhancement of the surrounding flow could increase the granule internal convection. A comparison between the shear rates of aerobic granules with primary particle sizes d_p of 1 and 10 μm in the flow fluid with different *Re* values indicates that the granule permeability could decrease the resistance caused by the surrounding flow to a certain degree.

Acknowledgments

The authors thank the Natural Science Foundation of China (50625825, 50738006, and 50828802), and the Key Special Program on the S&T for the Pollution Control and Treatment of Water Bodies (2008ZX07316-003 and 2008ZX07103-001) for the support of this study.

Notation

A = constant, dimensionless
d = granule diameter, m
d_p = the primary particle diameter, m
D = the fractal dimension of the aerobic granule sludge, dimensionless
D_L = the diameter of the calculation domain tube, m
f = the ratio of the wet mass to the dry mass of the aerobic granules, dimensionless
L = the length of the calculation domain tube, m
r_g = granule radius, m
S = shear rate, s^{-1}
u_8 = fluid velocity, m s^{-1}
$\vec{u}_f$ = the fluid velocity outside the granule, m s^{-1}
$\vec{u}_p$ = the fluid velocity within the porous granule, m s^{-1}
W_d = the wet mass of granule, g

Greek letters

β = permeability factor, dimensionless
ε = the porosity of the aerobic granules, dimensionless
ρ = density of the fluid, kg m^{-3}
ρ_g = density of the aerobic granules, kg m^{-3}
κ = the hydraulic permeability of the granule, cm^2
μ = fluid viscosity, Pa s

Literature Cited

1. Tay JH, Liu QS, Liu Y. Aerobic granulation in sequential sludge blanket reactor. *Water Sci Technol*. 2002;46:13–18.
2. Liu Y, Tay JH. State of the art of biogranulation technology for wastewater treatment. *Biotechnol Adv*. 2004;22:533–563.

3. de Kreuk MK, Pronk M, van Loosdrecht MCM. Formation of aerobic granules and conversion processes in an aerobic granular sludge reactor at moderate and low temperatures. *Water Res.* 2005;39: 4476–4484.
4. Zheng YM, Yu HQ, Sheng GP. Physical and chemical characteristics of granular activated sludge from a sequencing batch airlift reactor. *Process Biochem.* 2005;40:645–650.
5. Li AJ, Yang SF, Li XY, Gu JD. Microbial population dynamics during aerobic sludge granulation at different organic loading rates. *Water Res.* 2008;42:3552–3560.
6. McSwain BS, Irvine RL, Wilderer PA. The influence of-settling time on the formation of aerobic granules. *Water Sci Technol.* 2004;50:195–202.
7. Zhang JJ, Li XY, Oh SE, Logan BE. Physical and hydrodynamic properties of flocs produced during biological hydrogen production. *Biotechnol Bioeng.* 2004;88:854–860.
8. Li XY, Logan BE. Permeability of fractal aggregates. *Water Res.* 2001;35:3373–3380.
9. Xiao F, Yang SF, Li XY. Physical and hydrodynamic properties of aerobic granules produced in sequencing batch reactors. *Sep Purif Technol.* 2008;63:634–641.
10. Su KZ, Yu HQ. Formation and characterization of aerobic granules in a sequencing batch reactor treating soybean-processing wastewater. *Environ Sci Technol.* 2005;39:2818–2827.
11. Chu CP, Lee DJ. Multiscale structures of biological flocs. *Chem Eng Sci.* 2004;59:1875–1883.
12. Tsou GW, Wu RM, Yen PS, Lee DJ, Peng XF. Advective flow and floc permeability. *J Colloid Interface Sci.* 2002;250:400–408.
13. Yang Z, Peng XF, Lee DJ, Ay S. Advective flow in spherical floc. *J Colloid Interface Sci.* 2007;308:451–459.
14. Mu Y, Ren TT, Yu HQ. Drag coefficient of porous and permeable microbial granules. *Environ Sci Technol.* 2008;42:1718–1723.
15. Santos JLC, Geraldes V, Velizarov S, Crespo JG. Investigation of flow patterns and mass transfer in membrane module channels filled with flow-aligned spacers using computational fluid dynamics (CFD). *J Membr Sci.* 2007;305:103–117.
16. Favelukis M, Mudunuri R R. Unsteady mass transfer in the continuous phase around axisymmetric drops of revolution. *Chem Eng Sci.* 2003;58:1191–1196.
17. Diez L, Zima BE, Kowalczyk W, Delgado A. Investigation of multiphase flow in sequencing batch reactor (SBR) by means of hybrid methods. *Chem Eng Sci.* 2007;62:1803–1813.
18. Ren TT, Mu Y, Ni BJ, Yu HQ. Hydrodynamics of upflow anaerobic sludge blanket reactors. *AIChE J.* 2009;55:516–528.
19. Feng ZG, Michaelides EE. Unsteady heat and mass transfer from a spheroid. *AIChE J.* 1997;43:609–614.
20. Martin M, Montes FJ, Galan MA. Approximate theoretical solution for the Sherwood number of oscillating bubbles at different Reynolds numbers. *Chem Eng Prog.* 2010;49:245–254.
21. Neale GH, Nader WK. Prediction of transport processes within porous media: diffusive flow processes within an homogeneous swarm of spherical particles. *AIChE J.* 1973;20:530–538.
22. Li XY, Logan BE. Collision frequencies of fractal aggregates with small particles by differential sedimentation. *Environ Sci Technol.* 1997;31:1229–1236.
23. Li XY, Yuan YA. Settling velocities and permeabilities of microbial aggregates. *Water Res.* 2002;36:3110–3120.
24. Li DH, Ganczarczyk J. Advective transport in activated-sludge flocs. *Water Environ Res.* 1992;64:236–240.
25. Mu Y, Yu HQ. Biological hydrogen production in a UASB reactor with granules. I. Physicochemical characteristics of hydrogen-producing granules. *Biotechnol Bioeng.* 2006;94:980–987.
26. APHA. *Standard Methods for the Examination of Water and Wastewater*, 20th ed. Washington, DC: American Public Health Association, 1998.
27. Li DH, Ganczarczyk J. Fractal geometry of particle aggregates generated in water and wastewater treatment processes. *Environ Sci Technol.* 1989;23:1385–1389.
28. Bellouti M, Alves MM, Novais JM, Mota M. Flocs vs granules: differentiation by fractal dimension. *Water Res.* 1997;31:1227–1231.
29. Wu RM, Feng WH, Tsai IH, Lee DJ. An estimate of activated-sludge floc permeability: a novel hydrodynamic approach. *Water Environ Res.* 1998;70:1258–1264.
30. Adav SS, Chang CH, Lee DJ. Hydraulic characteristics of aerobic granules using size exclusion chromatography. *Biotechnol Bioeng.* 2008;99:791–799.
31. Tay JH, Li QS, Liu Y. The effects of shear force on the formation, structure and metabolism of aerobic granules. *Appl Microbiol Biotechnol.* 2001;57:227–233.

Manuscript received Jun. 26, 2010, revision received Aug. 26, 2010, and final revision received Oct. 13, 2010.